Measurement of the fourth moment of the current distribution in two-dimensional random resistor networks

M. A. Dubson* and Y. C. Hui

Department of Physics, The Ohio State University, Columbus, Ohio 43210

M. B. Weissman

Department of Physics, The University of Illinois, Urbana, Illinois 61801

J. C. Garland

Department of Physics, The Ohio State University, Columbus, Ohio 43210

Using a new experimental technique, we have measured the fourth moment of the current distribution in two-dimensional random resistor networks. The fourth moment is proportional to relative resistance fluctuations in a network of noisy resistors, and, until now, noise measurements provided the only experimental probe of this higher moment. We show that the fourth moment is simply related to the resistance change due to joule heating in a network of temperature-dependent resistors. We report measurements on both square-lattice and random-void continuum networks, fabricated by scribing computer-generated percolation patterns on sheets of aluminized Mylar.

I. INTRODUCTION

Critical exponents describing the divergence of topological quantities at the percolation threshold are universal in the sense that they depend only on the dimensionality of the system and not on system details. A topological exponent, such the correlation length exponent, is not sensitive to the lattice on which the percolation occurs nor to the distinction between lattice and continuum systems. In contrast, exponents associated with the higher moments of the current distribution in a random resistor network are generally system dependent.

Rammal et al.[1] and de Arcangelis et al.[2] have shown that the current distribution in a percolating resistor network is characterized by an infinite hierarchy of independent exponents, each exponent associated with a different moment of the current distribution. In general, the higher moments are more dependent upon nonuniversal aspects of system geometry. This dependence results from the domination of the higher moments by the weaker links, whose exact distribution is sensitive to details of the local geometry. The characterization of a system by such a hierarchy of exponents has been termed multifractility.[3]

Consider, for example, a random resistor network (Fig. 1) with total resistance R, carring a total current I, made up of elements of resistance r_α carrying currents i_α. By conservation of energy, we can write

$$R = (1/I^2) \sum_\alpha i_\alpha^2 r_\alpha \; ,$$

and we observe that resistance measurements probe the second moment of the current distribution. Near the percolation threshold, the resistance obeys a power law, $R \simeq (p - p_c)^{-t}$, where p is the concentration, p_c is the critical concentration, and t is the conductivity exponent. It is the second moment of the current distribution which contains the divergence at p_c and the exponent t. Similarly, in networks of noisy resistors, one can show that measurements of resistance noise probe the fourth moment of the current distribution.[1] The relative resistance noise in such a network diverges near the percolation threshold with a nonuniversal exponent κ as

$$\langle \Delta R^2 \rangle / R^2 \simeq (p - p_c)^{-\kappa} \; .$$

This divergence of the resistance noise near p_c has been seen in a number of measurements of $1/f$ noise in percolating metal-insulator systems[4-8] and may be understood intuitively as follows.[9] Far above the percolation threshold, there exist many current paths in parallel.
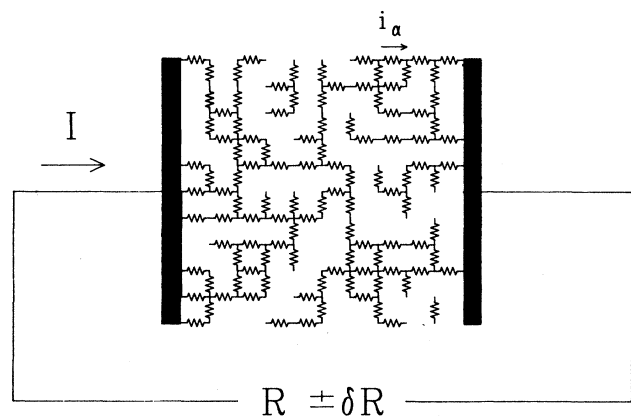
FIG. 1. Discrete random resistor network.

Each current path is noisy, but since the noise on different paths is uncorrelated, the fluctuations tend to average out. Closer to threshold, only a few paths carry the current, the averaging is less complete, and the relative resistance noise is larger. In a finite discrete network, the divergence is cut off by finite-size effects. The relative resistance noise of the system cannot exceed that of a single element and, in fact, it saturates at a lower level.[1]

Recently, the transport properties of random-void (or "Swiss-cheese") continuum systems has been a subject of active investigation.[10] A random-void system consists of a uniform metallic medium randomly peppered with insulating voids. In general, the values of the exponents t and κ are sensitive to the distribution of constrictions between voids, which in turn depends on the shape of the voids. An exception to this rule is the exponent t in two dimensions (2D), which happens not to depend on the void shape and has the same value[11] ($t = 1.30 \pm 0.01$) as in lattice systems. However, the noise exponent κ, which probes a higher moment, is extremely sensitive to details of the geometry. Both analytic arguments and numerical simulations[1,7,9] yield $\kappa = 1.12 \pm 0.02$ for 2D discrete lattice networks and $4.12 < \kappa < 5.02$ for the 2D random-void system with circular voids.

Attempts to determine κ in 2D random-void systems by measuring $1/f$ noise in discontinuous metal films yield a wide range of values. Koch et al.[6] report $\kappa = 2.6 \pm 0.2$ in ion-milled gold films. Garfunkel and Weissman[7] measure $\kappa = 7.8 - 9.1$ in sandblasted aluminum, indium, and chromium films. Garfunkel and Weissman argue, however, that inhomogeneities in their samples result in an artificially high value of κ, and that, after an appropriate correction, their best value is $\kappa \simeq 5$. Octavio et al.[8] report $\kappa = 2.7 \pm 0.3$ in ion-milled silver films. While all of these experiments yielded values of κ significantly higher than the lattice value, detailed interpretation of the results is hampered by the poorly known morphology of the sample films.

In this paper we present measurements of the fourth moment of the current distribution in 2D random resistor networks. Using a new technique, which involves the thermal response of the network to an external current, we determine the fourth moment directly, without the need for a measurement of resistance noise. Our 2D resistor networks consist of sheets of aluminized mylar on which are scribed computer-generated percolation patterns—both lattice and random-void continuum patterns. Because the patterns are computer generated, the sample morphology is well characterized.

We emphasize that this new technique allows measurement of the fourth moment of the current distribution in a system in which a measurement of resistance noise is impossible. Our samples are so large that $1/f$ noise (which scales inversely as sample volume) is unmeasurably small, being orders of magnitude smaller than the Johnson noise in the system at practicable current levels.

This paper is organized as follows. In Sec. II we show that the fourth moment of the current distribution in a network of temperature-dependent resistors can be deduced from measurements of system's resistance change arising from joule heating. In Sec. III and the Appendix, we describe our samples and the ac bridge circuit that measures thermally induced resistance oscillations. Also in Sec. III, we calculate the amplitude of the temperature and resistance oscillations for a particularly simple geometry—a rectangular sheet—and compare the calculation with measurements. Our data on random networks, both lattice and continuum, and comparisons with theory are presented in Sec. IV, along with a discussion of finite-size effects. Finally, in Sec. V, we describe some unusual features of the square-hole random-void continuum system, which was chosen for experimental convenience. We argue that unusual fluctuation effects in this system may make the critical regime experimentally inaccessible.

II. THEORY OF THERMAL RESPONSE

Here we show how resistance changes arising from joule heating in a random resistor network are related to the fourth moment of the current distribution. The connection between thermal response and resistance fluctuations was first recognized by Weissman and Dollinger.[12] Resistance noise and the fourth moment are dominated by the system's weak links through which much of the sample current is channeled. These same weak links dominate the system's thermal response, since joule heating is greatest there.

Consider again the random discrete resistor network shown in Fig. 1. Each network element α has a mean resistance r_α and a resistance noise $\langle \delta r_\alpha^2 \rangle$, the angle brackets $\langle \rangle$ indicating a time average within some bandwidth in frequency space. Resistance fluctuations of different elements are assumed to be uncorrelated, i.e.,

$$\langle \delta r_\alpha \delta r_\beta \rangle = \delta_{\alpha\beta} \langle \delta r_\alpha^2 \rangle .$$

The mean total resistance of the entire network (as measured either between two nodes in the network or, as in Fig. 1, between two borders) is R. The network carries a total current I with i_α defined as the current in element α.

By Tellegen's theorem,[1] the relative resistance noise $S_R = \langle \delta R^2 \rangle / R^2$ is given by

$$\frac{\langle \delta R^2 \rangle}{R^2} = \frac{\sum_\alpha i_\alpha^4 \langle \delta r_\alpha^2 \rangle}{\left[\sum_\alpha i_\alpha^2 r_\alpha \right]^2} . \tag{1}$$

If all of the elementary resistors r_α have the same mean resistance r and the same noise $\langle \delta r^2 \rangle$, then Eq. (1) factors as

$$S_R = \frac{\langle \delta r^2 \rangle}{r^2} \frac{\sum_\alpha i_\alpha^4}{\left[\sum_\alpha i_\alpha^2 \right]^2} . \tag{2}$$

The first factor $\langle \delta r^2 \rangle / r^2$ is the relative resistance noise of each (identical) element and depends on the microscopic mechanism of resistance noise generation in the system under consideration. The second term, which is

purely geometrical, contains the divergence at p_c and the exponent κ:

$$\frac{\sum_{\alpha} i_{\alpha}^4}{\left[\sum_{\alpha} i_{\alpha}^2\right]^2} \sim (p-p_c)^{-\kappa}, \quad p \text{ near } p_c \, . \tag{3}$$

We can argue similarly for the Swiss-cheese continuum case. The irregularly shaped conducting paths in the Swiss-cheese system can be regarded as consisting of a fine mesh of identical, discrete resistors. In the limit that the mesh size is very small compared to the size of the holes in the system, the continuum system is accurately modeled by a discrete lattice network. Equation (1), now applied to this fine grid of resistors, again factors as in Eq. (2). More generally, all arguments made below referring to discrete resistor networks apply equally well to continuum systems.

Note that expression (2) for the relative resistance noise has the form of the inverse participation ratio. For an $L \times L$ resistor network, with fill fraction $p = 1$ and carrying a total current I, i_{α} is either I/L or 0 according to whether the bond α is parallel or perpendicular to the current flow. In this case,

$$\sum_{\alpha} i_{\alpha}^4 \bigg/ \left[\sum_{\alpha} i_{\alpha}^2\right]^2 = [(L^2/2)(I/L)^4]/[(L^2/2)(I/L)^2]^2$$

$$= 1/(L^2/2) \, .$$

In the extreme case that a single element dominates the sums in (2), we would have

$$\sum_{\alpha} i_{\alpha}^4 \bigg/ \left[\sum_{\alpha} i_{\alpha}^2\right]^2 \simeq 1 \, .$$

This would occur in a system with a single narrow constriction through which all the sample current is funneled. In general,

$$\sum_{\alpha} i_{\alpha}^4 \bigg/ \left[\sum_{\alpha} i_{\alpha}^2\right]^2 \simeq 1/N \, ,$$

where N is the number of bonds which contribute significantly to the total noise.

Consider now a resistor network carrying an ac current $I = I_0 \cos(\omega t)$ with each element α carrying a current $i_{\alpha} \cos(\omega t)$. Assuming that the resistors have a positive temperature coefficient of resistance, joule heating will increase both the temperature and the resistance of each current-carrying element. The power dissipated in resistor r_{α} is

$$i_{\alpha}^2 r_{\alpha} \cos^2(\omega t) = \frac{i_{\alpha}^2 r_{\alpha}}{2}[1 + \cos(2\omega t)] \, . \tag{4}$$

Assuming linear response, the ac component of this power at frequency $f = 2\omega$ causes temperature oscillations at $f = 2\omega$ of amplitude ΔT_{α}. In the steady state, the temperature of element α can be written as

$$T_{\alpha} = T_{\alpha 0} + \Delta T_{\alpha} \cos(2\omega t + \phi) \, , \tag{5}$$

where ϕ is the phase shift between power and temperature oscillations. Both the amplitude ΔT_{α} and phase

shift ϕ depend on the details of the thermal response of the resistor network; i.e., the thermal coupling between the resistors and their environment, their heat capacity, etc.

At this point, we make the crucial assumption that ΔT_{α} is proportional to the local power generation and write

$$\Delta T_{\alpha} = i_{\alpha}^2 r_{\alpha} h(\omega) \, , \tag{6}$$

where $h(\omega)$ is some function of frequency but not of α. We will argue below that this assumption is valid for our experimental system.

From Eqs. (5) and (6), r_{α} can be written

$$r_{\alpha} = r_{\alpha 0} + \Delta r_{\alpha} \cos(2\omega t + \phi) \, , \tag{7}$$

with

$$\Delta r_{\alpha} = \beta r_{\alpha} \Delta T_{\alpha} = \beta i_{\alpha}^2 r_{\alpha}^2 h(\omega) \, . \tag{8}$$

Here,

$$\beta \equiv (1/r_{\alpha})(dr_{\alpha}/dT)$$

is the temperature coefficient of resistance, assumed equal for all resistors α.

The network resistance $R = R(r_{\alpha})$ consequently oscillates at $f = 2\omega$ with amplitude

$$\Delta R = \sum_{\alpha} \frac{\partial R}{\partial r_{\alpha}} \Delta r_{\alpha} \, . \tag{9}$$

We now invoke Cohen's theorem[1,13] which states that $\partial R/\partial r_{\alpha} = i_{\alpha}^2/I^2$. This theorem and Eqs. (8) and (9) lead to

$$\Delta R = \frac{\beta h(\omega)}{I^2} \sum_{\alpha} i_{\alpha}^4 r_{\alpha}^2 = \frac{\beta h(\omega) r^2}{I^2} \sum_{\alpha} i_{\alpha}^4 \, . \tag{10}$$

(In the last step we have once again assumed $r_{\alpha} = r$ for all α.)

We conclude that the amplitude of the resistance oscillation at frequency 2ω, resulting from an ac current at frequency ω, is proportional to the fourth moment of the current distribution. This conclusion is valid for both discrete and continuum systems so long as the amplitude of the local temperature oscillation is proportional to the amplitude of the local joule power generated.

III. EXPERIMENT

Our experimental system is a sheet of aluminized Mylar plastic,[14] 0.005 in. thick, covered with a uniform 500-Å aluminum film. The sheet resistance of the film is approximately 2 $\Omega/\square$ and varies by less than 0.1% over a 30×30 cm^2 sample.

Using a technique described previously,[15] we use a "hot needle" to scribe a percolating pattern in the film with a computer-controlled digital plotter. When the hot needle draws a square, the interior of the square is electrically disconnected from the exterior. As far as current flow is concerned, it is as if a hole were punched in the sheet. Two types of patterns were studied: a square-lattice pattern and a random-void continuum system con-

sisting of square holes with parallel-oriented edges as shown in Fig. 2. Typically, the lattice size was 100×100 and the sample resistance varied from $\simeq 2 \ \Omega$ for an unbroken sheet to $\simeq 200 \ \Omega$ for patterns near the percolation threshold.

The square holes of the square-lattice samples touch at the corners. As shown in Fig. 2, corner contact between square holes is guaranteed by short diagonal cuts added at the corners where the squares touch. The uncut sites thus form a percolating network with first-nearest-neighbor contact only. The program that generates the square-lattice pattern selects new sites at random but does not repeat previously drawn sites. In the continuum case, square sites are located at random with no underlying background lattice, independently of previously drawn sites. The sites are thus freely interpenetrating.

This aluminized Mylar technique was used previously to study the conductivity of square-lattice and random-void continuum systems.[15] The measured conductivity exponent and critical concentration for the lattice system agreed very well with the results known from Monte Carlo studies, and, to within experimental uncertainties, the conductivity exponents for the lattice and continuum systems were identical, as predicted by theory.[10]

We made several unsuccessful attempts to cut circular holes in order to study the true "Swiss-cheese" continuum case which has been well studied theoretically.[10] Two difficulties were encountered which made this impossible. The first problem was that the digital plotter could only make straight lines, and so approximated circles with many-sided polygons. The drawing of such polygons was both considerably slower and mechanically less perfect than the drawing of squares, resulting in poorly defined sample geometries. A second experimental problem, which was never clearly resolved, was that round-hole patterns exhibited a puzzling frequency-dependent thermal response. As explained below, the amplitude of the joule-heating-induced resistance oscillation should scale with frequency ω of the ac current as $(1/\omega)^{1/2}$. In-

stead, we frequently saw a $(1/\omega)^{(0.3-0.4)}$ dependence, leading to ambiguous results.
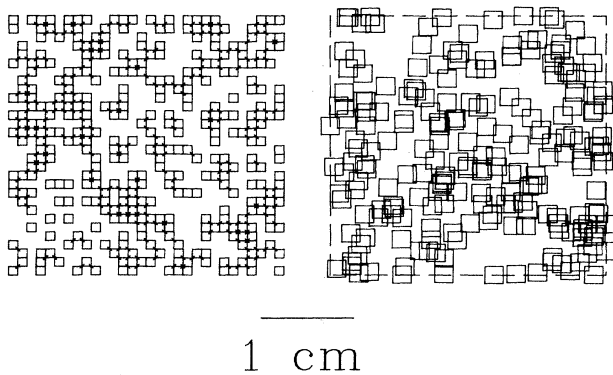
As the percolating pattern is cut by the plotter, the fourth moment of the current distribution is measured with the bridge circuit shown in Figs. 3 and 8, and described in the Appendix. The circuit is similar to the ac double Kelvin bridge often used in cryogenic thermometry[16] and resembles a circuit used recently to investigate the thermal response of glasses.[17]

In this circuit, an ac current at frequency $\omega (\omega \simeq 35$ Hz) excites a voltage response at frequency 3ω. As described in Sec. II, with a sample current $I = I_0 \cos(\omega t)$, joule heating causes the sample's resistance to oscillate at 2ω:

$$R = R_0 + \Delta R \cos(2\omega t + \phi) \ . \tag{11}$$

Typically, $\Delta R \ll R_0$. The sample voltage is thus

$$V = IR \simeq I_0 R_0 \cos(\omega t) + \tfrac{1}{2} I_0 \Delta R \cos(3\omega t + \phi) \ . \tag{12}$$

[The difference frequency term, $\tfrac{1}{2} I_0 \Delta R \cos(\omega t + \phi)$, is overwhelmed by the large $I_0 R_0$ term and is ignored.]

The voltage in Eq. (12) consists of a large component (typically $\simeq 0.1 - 1$ V) at frequency ω and a small component ($\simeq 1 - 100 \ \mu$V) at frequency 3ω. As shown in the Appendix, when the bridge is balanced, the large ω component is nulled, and the remaining 3ω component at the bridge output has amplitude $V_{3\omega} = \tfrac{1}{4} I_0 \Delta R$ (an extra factor of $\tfrac{1}{2}$ is introduced by the bridge circuitry).

The quantity we seek, $\sum_\alpha i_\alpha^4 / (\sum_\alpha i_\alpha^2)^2$, is related to the 3ω component $V_{3\omega}$, the amplitude of the sample current I_0, and the sample resistance R, by

$$S_R \propto \frac{\sum\limits_\alpha i_\alpha^4}{\left[\sum\limits_\alpha i_\alpha^2 \right]^2} \propto \frac{V_{3\omega}}{I_0^3 R^2} \ . \tag{13}$$

This result follows from Eq. (10) and the conservation of energy relation

$$I^2 R = \sum_\alpha i_\alpha^2 r_\alpha = r \sum_\alpha i_\alpha^2 \ .$$

(Again, we take $r_\alpha = r$ for all α.)

A few comments on the bridge circuit are in order.

1 cm

FIG. 2. Scale reproductions of percolation patterns that were scribed on aluminized Mylar sheets. The square-lattice pattern is on the left and the random-void continuum pattern with square holes is on the right. Both patterns are shown at the critical hole concentration.
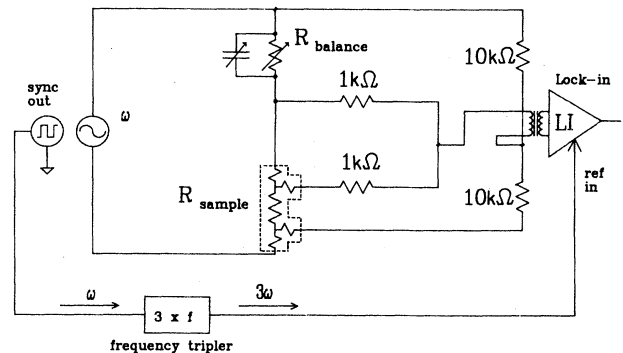
FIG. 3. Bridge circuit.

The bridge arrangement relaxes the requirement for extreme spectral purity in the signal source. Any 3ω component from the source appears across both arms of the bridge and, like the ω component, is balanced out. Only the 3ω signal arising from joule heating unbalances the bridge and produces a signal at the output.

The signal source is 10-W audio amplifier driven by a frequency synthesizer operated at a frequency of about 35 Hz. To achieve a bridge balance of 1 part in 10^5, the capacitive component of the sample plus leads ($<0.1\mu F$) is nulled with a variable capacitor in parallel with the balance resistor. The 1-kΩ resistors in Fig. 3 are large compared to the contact resistances to the sample, thus ensuring that the same current flows in sample and balance resistor and that negligible current flows along the voltage leads. The 10-kΩ resistors are large compared to the sample resistance so that most of the source current flows through the balance resistor and sample. The frequency tripler uses a phase-locked loop circuit.[18]

As shown in Fig. 3, the bridge output must be transformer coupled to the lock-in in order to eliminate the large common-mode signal which would saturate the lock-in input. Care was taken to ensure that the source impedance is such that the transformer provides a flat transfer ratio over the frequency range of interest. The output impedance of the bridge in Fig. 3 is 5500 Ω. With this source impedance, our transformer, a G-10 Triad Geoformer, provides flat gain from 5 Hz to more than 1 kHz.

We turn now to a calculation of the magnitude of the resistance oscillation in our aluminized Mylar sheets. The thin aluminum film on the thick Mylar sheet may be modeled as a 2D heat source on a semi-infinite substrate with the substrate characterized by a thermal conductivity κ and a heat capacity per unit volume c_v. The aluminum film is so thin ($\simeq 500$ Å) that its heat capacity is negligible. Consider a film of length L, width W, and negligible thickness, carrying a current $I\cos(\omega t)$ along its length. The film, at $z=0$, rests on a thick substrate which fills the half-space $z>0$. The power/unit area generated in the film is

$$\frac{I^2 R}{LW}\cos^2(\omega t)=j[1+\cos(2\omega t)] \, , \qquad (14)$$

where $R=R_\square L/W$ is the film resistance and $j=I^2 R/(2LW)$ is the average power/unit area dissipated.

Neglecting edge effects and the heat capacity of the thin film, we solve the 1D heat-flow equation with the boundary condition that the heat flux at the surface $z=0$ is given by (14). The time-dependent part of the solution is a damped temperature wave[19]

$$T(z,t)=\Delta T e^{-z/\delta}\cos\left[2\omega t-\frac{z}{\delta}+\frac{\pi}{4}\right] , \qquad (15)$$

$$\Delta T=\frac{j}{(2\omega\kappa c_v)^{1/2}}=\frac{I^2 R}{(2LW)}\frac{1}{(2\omega\kappa c_v)^{1/2}} \, .$$

Here, $\delta=[\kappa/(\omega c_v)]^{1/2}$ is the thermal penetration depth. At $z=0$, the temperature oscillations lag power oscilla-

tions by $\pi/4$. So long as δ is small compared to L, W, and the thickness of the substrate, edge effects can be neglected and our 1D analysis is valid. At frequency $f\simeq35$ Hz, where much of our data was obtained, $\delta\simeq20$ μm. The thickness of the Mylar sheet is 0.005 in. $=130$ μm, which is sufficiently large compared to δ to approximate a semi-infinite substrate with negligible error.

The resistance oscillation of the film resulting from temperature oscillation of amplitude ΔT is

$$\Delta R =\beta R \Delta T=\frac{I^2 R^2}{2(2\kappa c_v)^{1/2}}\frac{\beta}{LW}\frac{1}{\omega^{1/2}} . \qquad (16)$$

The measured value of β, the temperature coefficient of resistance, for our aluminum film samples is 0.0017 K^{-1}. As shown in the Appendix, the 3ω component of the voltage at the output of the bridge has amplitude $V_{3\omega}=I\Delta R/4$, which becomes, using Eq. (16)

$$V_{3\omega}=\frac{I^3 R^2}{8(2\kappa c_v)^{1/2}}\frac{\beta}{LW}\frac{1}{\omega^{1/2}}=\frac{I^3 R_\square^2}{8(2\kappa c_v)^{1/2}}\frac{\beta L}{W^3}\frac{1}{\omega^{1/2}} . \qquad (17)$$

Figure 4 is a plot of $V_{3\omega}/I^3$ versus frequency for a rectangular sample. Our measurements of $V_{3\omega}$ in rectangular samples show the dependence on I, L, W, and ω expected from Eq. (17), as well as the $\pi/4$ phase shift between power and resistance oscillations. In particular, the $1/(\omega)^{1/2}$ frequency dependence is clearly seen in Fig. 4. However, the measured magnitude of $V_{3\omega}$ is about 50% smaller than that predicted by Eq. (17) using literature values for κ and c_v of Mylar and our measured value of β. The reason for this discrepancy is not clear, but may be due to inaccurate values for κ and c_v.

The results of this 1D analysis can only be applied to our percolation patterns if all geometrical length scales in the patterns are large compared to the thermal penetration depth δ. However, occasional narrow necks which arise in the random-void patterns may have widths comparable to or smaller than δ. If such necks contribute significantly to the fourth moment of the current distribution, the 1D analysis given above is invalid, and one would not see a $\omega^{-1/2}$ frequency dependence in $V_{3\omega}$. The
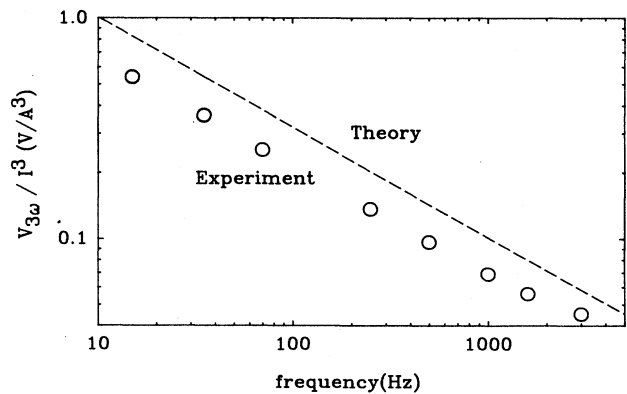
FIG. 4. $V_{3\omega}/I^3$ vs frequency for a simple rectangular sample (no voids).

DUBSON, HUI, WEISSMAN, AND GARLAND

$\omega^{-1/2}$ behavior was observed in all our square-hole random-void patterns at all fill fractions. We take this as strong evidence that the rare narrow necks with widths less than δ do not affect our results. Extremely narrow necks are not expected to contribute significantly to the fourth moment because such necks have very high resistance and so the current through them is squeezed off.[7] The failure of round-hole random-void patterns to exhibit the $\omega^{-1/2}$ frequency dependence may well be due to the importance of narrow necks and the consequent breakdown of our assumptions in that case.

IV. EXPERIMENTAL RESULTS

Figure 5 is a log-log plot of the noise parameter $V_{3\omega}/(R^2I^3)$ versus the hole concentration parameter $(f_c-f)/f_c$ for both the lattice and square-void continuum cases. f is the area fraction of insulator and f_c is the critical area fraction. $[(f_c-f)/f_c=(p-p_c)/(1-p_c)$, where p is the metal area fraction.] Displayed in the figure are data from five trials of a 100×100 lattice and three trials of the continuum case for samples of size $L/c=100$, where L is the sample edge length and c is the hole edge length.

For the lattice case, $f\propto N$ where N is the number of square holes cut and f_c is known from Monte Carlo studies[20] ($f_{c,\text{lattice}}\simeq0.40723$). For the continuum case, f and N are related by[21]

$$f(N)=1-e^{-Na/A},\qquad(18)$$

where a is the area of an individual void and A is the sample area. [We note that Eq. (18) holds regardless of the shape of the void if the void positions are uncorrelated.] From previous measurements,[15] the square-void continuum system has a critical void fraction of $f_c=0.61\pm0.01$.

Figure 6 is a semilog plot of $V_{3\omega}/(R^2I^3)$ versus metal area fraction p. The data shown are the averages of the
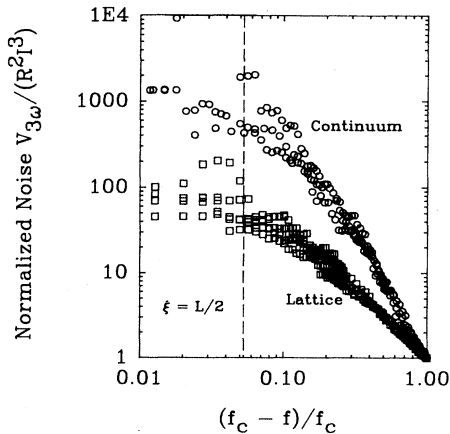
FIG. 6. Semi-log plot of "noise" vs concentration p for square-lattice and continuum systems. p is the metal area fraction; f is the insulator area fraction.

trials displayed in Fig. 5. Note that the two curves, lattice and continuum, coalesce in the dilute regime at $p>0.7$. The corresponding data sets in Fig. 5 do not appear to overlap at high p (low f) because f_c is different for the two systems.

Because of finite-size effects in our small systems, it is very difficult to extract reliable values for the noise exponent κ. In a finite-sized system, critical power-law behavior is obeyed over a possibly narrow range in concentration p, bounded by finite-size effects close to the critical concentration p_c and by corrections to scaling away from p_c. We have fit the data in Fig. 5 to a power law

$$V_{3\omega}/(R^2I^3)\propto(f_c-f)^{-\kappa}$$

over the range bounded by the conditions $(f_c-f)/f_c=0.3$ and $\xi=L/2$ (shown as dashed vertical line in Fig. 5). ξ is the correlation length for the lattice case and L is the size of system. In units of the lattice constant, $L=100$ and ξ is taken[22] to be $[f_c/(f_c-f)]^{4/3}$. A least-squares fit over this somewhat arbitrarily chosen window yields

$$\kappa_{\text{Lattice}}=1.49\pm0.06$$

and

$$\kappa_{\text{Continuum}}=2.6\pm0.2\ .$$

In each case, the assigned uncertainty is twice the standard deviation of the mean.

For the square lattice case, κ has been established with high confidence by Monte Carlo simulations[1] and has been set at $\kappa=1.12\pm0.02$. In addition, analytic arguments[23] provide rigorous upper and lower bounds on κ: $1.08<\kappa<1.37$. The discrepancy between our estimate of κ and the value predicted by theory indicates that our system is not large enough to provide an adequate scaling regime.

FIG. 5. Log-log plot of the noise parameter $V_{3\omega}/(R^2I^3)$ vs the hole concentration parameter $(f_c-f)/f_c$ for square lattice and square-void continuum cases. f is the area fraction of insulator.

As outlined in Sec. V, the calculation of κ for the case of continuum square voids is quite delicate, with unusual fluctuation effects predicted. With the caveats described below, the predicted value is $\kappa = 3.4 \pm 0.3$, higher than our measured value. Again, we take the discrepancy to mean that our system is too small to observe undistorted critical behavior.

As seen in Fig. 5, finite-size effects cut off the noise divergence close to f_c. Rammal et al.[1] predict that near f_c for $\xi \gg L$, the relative resistance noise $S_R(p)$ will saturate at

$$S_R(p)/S_R(p=1) \simeq L^{\kappa/\nu} ,$$

where ν is the correlation exponent ($\nu = \frac{4}{3}$ in 2D). Taking $\kappa = 1.1$ for the lattice case and $L = 100$, our lattice noise is expected to saturate at $100^{(1.1/1.33)} \simeq 50$, approximately the observed value. The continuum case, with a higher κ, is expected to saturate at a higher value, as observed in our data; however, the peculiar nature of the square-void system (see Sec. V) makes a quantitative prediction difficult.

V. DISCUSSION AND SUMMARY

In continuum percolation the exponent for the divergence of the noise magnitude near the percolation threshold deviates from the standard lattice value $\kappa \simeq 1.12$ because near p_c small, noisy necks are forced to carry current. This deviation depends on both the distribution of resistances of narrow necks in the continuum conductor and on the scaling of the noise magnitude in a neck with its resistance. Both of these factors are highly nonuniversal in that they depend on the details of the percolation geometry. In the case of 2D random-void geometry with circular holes, convincing arguments[7] indicate $4.12 < \kappa < 5.02$. We shall see that when the circular holes are replaced with squares, the same value of κ is predicted, but with some peculiar statistical effects which are expected to reduce the value of κ observed in small or moderately sized systems. These unusual effects are due to the importance of rare small necks.

Unlike nearby circles, whose spacing is described by a single length, two nearby squares (with the same orientation) must be characterized both by their separation a and their overlap length b as shown in Fig. 7. As a result, there is no simple scaling of noise with neck resistance, since different shaped necks can have the same resistance. This feature will lead to the complications described here.

Letting both the sheet resistance and the edge length of a square be unity, the resistance formed by the neck is $r \simeq (b/a) + (4/\pi)\ln(1/a)$, where the first term is the obvious internal neck resistance and second is approximately the spreading resistance required to squeeze the field lines into the channel. We are not attempting here to keep dimensionless factors which do not affect the qualitative conclusion. By arguments given previously,[7] such a neck will carry about the typical neck current so long as $r < r_m$, where r_m is somewhere between the typical node-to-node resistance and the node-to-node resistance of the singly connected links alone. Thus r_m scales as
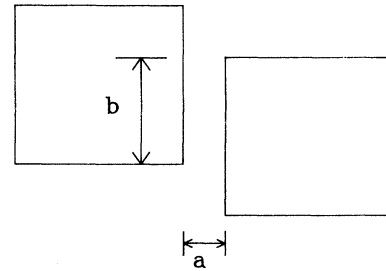
FIG. 7. Square-void geometry.

$$(p - p_c)^{-w} = \Delta^{-w} ,$$

where $1 < w < t \simeq 1.30$. For $r > r_m$, the current through the neck is inversely proportional to r, so that such weak links are relatively unimportant.

Using the standard assumption that the fractional resistance fluctuations are inversely proportional to area, we find that the leading term in $\langle \delta r^2 \rangle$ should be b/a^3. The average link noise then increases as Δ goes to zero as

$$\int_{a > a_m} \int_{b > a}^{b = ar_m} \left[\frac{b}{a^3} \right] db \, da \simeq \int_{a_m}^{1} \frac{1}{a} (r_m^2 - 1) da$$

$$= (r_m^2 - 1)\ln(1/a_m) ,$$

where a_m is the width for which the spreading resistance alone is r_m, $\ln(1/a_m) \simeq r_m$. We have neglected necks with $b < a$, which makes a less divergent contribution. The leading term of the integral is

$$r_m^2 \ln(1/a_m) \simeq r_m^3 ,$$

which scales as Δ^{-3w}. Thus the correction to κ from continuum effects is $3w = 3.45 \pm 0.45$, as for circles. However, the path to this ordinary-seeming critical exponent is peculiar, since it includes an exponentially small cutoff in the neck width together with a logarithmic dependence on that cutoff.

The peculiarity of the square-continuum problem becomes even clearer when we look at the divergence of the eighth moment of the current distribution, which appears in the sample-to-sample variation of the noise magnitude. In this case the integrand must be replaced by (b/a^7), and the leading term of the integral becomes $r_m^2 \exp(\pi r_m)$. This diverges faster than any power law, and thus cannot be characterized by any critical exponent. We believe that such a result for a current density moment in a simple percolation problem has not previously been anticipated. In this problem, exponential divergences occur for all current moments higher than the fourth.

Two experimentally important consequences emerge. The first is that one of the factors of Δ^{-w} in the continuum correction results from exponentially improbable necks, and thus is unlikely to be found often in smallish experiments or simulations. Thus the expected observed κ is about $1.12 + 2w \simeq 3.4 \pm 0.3$. The second conclusion is more troubling. When the variance in a quantity diverges much faster than the square of the quantity, the

critical region cannot be approached too closely in any finite sample. The measurement of a true κ for square-hole-continuum percolation may be intrinsically nearly impossible, since it would seem to require exponentially large averaging areas.

One other unusual feature of square voids, which does not seem to affect our conclusions, is that the current density around an isolated square diverges near the corners. The current density at a distance ρ from a right angle corner diverges as $\rho^{-1/3}$ (Ref. 24). The resulting fourth moment of the current density does not diverge, however. Hence, the sharp corner makes a finite contribution to the noise.

In summary, using a new experimental technique, we have measured the fourth moment of the current distribution in a 2D resistor network. Previously, resistance noise measurements provided the only experimental probe of this higher moment, and as a consequence, only resistor networks with suitably high $1/f$ resistance noise could be probed. Our technique relies on the thermal response of the network to an external ac current and gives a direct measure of the fourth moment even in a noiseless system. We have measured the fourth moment in 2D square-lattice and random-void continuum resistor networks fabricated by scribing computer-generated percolation patterns on aluminized Mylar sheets. As predicted by theory, we find that the random-void system has a higher fourth moment (higher "noise") than the lattice system near the percolation threshold. Although our results are in qualitative agreement with theory, our measured values of the noise exponent κ fall outside the bounds provided by numerical and analytical calculations, a discrepancy we tentatively attribute to finite-size effects.

ACKNOWLEDGMENTS

APPENDIX: OPERATION OF BRIDGE CIRCUIT

A schematic of the bridge circuit is shown in Fig. 8. The sample resistance is R_S, and R_B is an adjustable balance resistance. Current leads on the sample have con-
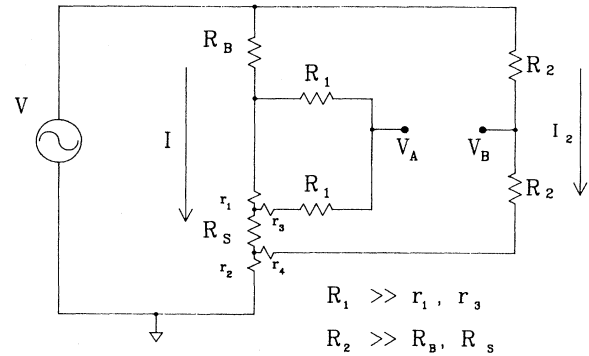
FIG. 8. Bridge circuit operation.

tact resistances r_1 and r_2, while the voltage leads have contact resistances r_3 and r_4. We assume $R_1 \gg r_1$ so that negligible current flows through the R_1-R_1-r_3 chain and nearly the same current I flows through R_B, r_1, and R_S. We also assume $R_1 \gg r_3$ and $R_2 \gg r_4$. Finally, we assume $R_2 \gg R_B, R_S$ so that most of the current from the source flows through the sample (we want $I_2 \ll I$). Note that the current through r_2 is $I + I_2$. The voltages V_A and V_B at the outputs are then

$$V_A = (I + I_2)r_2 + IR_S + \tfrac{1}{2}Ir_1 , \qquad (A1)$$

$$V_B = (I + I_2)r_2 + \tfrac{1}{2}I(R_S + r_1 + R_B) . \qquad (A2)$$

The output of the bridge is then

$$V_A - V_B = \tfrac{1}{2}I(R_S - R_B) . \qquad (A3)$$

When the bridge is balanced, the sample resistance may be written as

$$R_S = R_B + \Delta R \cos(2\omega t + \phi) , \qquad (A4)$$

where, as explained in Sec. II, the ac part of the sample resistance is due to joule heating. Writing the sample current as $I = I_0 \cos(\omega t)$, we have from (A3) and (A4),

$$V_A - V_B = \tfrac{1}{2}I_0 \cos(\omega t) \times \Delta R \cos(2\omega t + \phi)$$

$$\simeq \tfrac{1}{4}I_0 \Delta R \cos(3\omega t + \phi) + \tfrac{1}{4}I_0 \Delta R \cos(\omega t + \phi) .$$

$$(A5)$$

*Present address: Dept. of Physics and Astronomy, Michigan State University, East Lansing, MI 48824.

[1]R. Rammal, C. Tannous, P. Breton, and A.-M. S. Tremblay, Phys. Rev. Lett. 54, 1718 (1985); R. Rammal, C. Tannous, and A.-M. S. Tremblay, Phys. Rev. A 31, 2662 (1985).

[2]L. de Arcangelis, S. Redner, and A. Coniglio, Phys. Rev. B 31, 4725 (1985); 34, 4656 (1986).

[3]Time-Dependent Effects in Disordered Materials, Vol. 167 of NATO Advanced Study Institute, Series B: Physics, edited by R. Pynn and T. Riste (Plenum, New York, 1987), pp.

145–193.

[4]D. A. Rudman, J. J. Calabrese, and J. C. Garland, Phys. Rev. B 33, 1456 (1986).

[5]Joseph V. Mantese and Watt W. Webb, Phys. Rev. Lett. 55, 2212 (1985).

[6]R. H. Koch, R. B. Laibowitz, E. I. Alessandrini, and J. M. Viggiano, Phys. Rev. B 32, 6932 (1985).

[7]G. A. Garfunkel and M. B. Weissman, Phys. Rev. Lett. 55, 296 (1986).

[8]Miguel Octavio, Gustavo Gutierrez, and Juan Aponte, Phys.

Rev. B **36**, 2461 (1987).

[9]David C. Wright, David J. Bergman, and Yacov Kantor, Phys. Rev. B **33**, 396(1) (1986).

[10]B. I. Halperin, Shechao Feng, and P. N. Sen, Phys. Rev. Lett. **54**, 2391 (1985); Phys. Rev. B **35**, 197(1) (1987).

[11]D. J. Frank and C. J. Lobb, Phys. Rev. B **37**, 302 (1988); J. G. Zabolitzky, *ibid.* **30**, 4077 (1984); H. J. Herrmann, B. Derrida, and J. Vannimenus, *ibid.* **30**, 4080 (1984); D. C. Hong, S. Havlin, H. J. Herrman, and H. E. Stanley, *ibid.* **30**, 4083 (1984); C. J. Lobb and D. J. Frank, *ibid.* **30**, 4090 (1984).

[12]Michael B. Weissman and Gavin D. Dollinger, J. Appl. Phys. **52**(5), 3095 (1981).

[13]R. M. Cohn, Ann. Math. Soc. **1**, 316 (1950).

[14]The material, called "Mirrored Mylar" is sold by Ohio Graphics Arts, 26055 Every Rd., Cleveland, OH 44120.

[15]Michael A. Dubson and James C. Garland, Phys. Rev. B **32**, 7621 (1985).

[16]E. Zair and A. J. Greenfield, Rev. Sci. Instrum. **44**, 695 (1973).

[17]N. O. Birge and S. R. Nagel, Rev. Sci. Instrum. **58**, 1464 (1987).

[18]Paul Horowitz and Winfield Hill, *The Art of Electronics* (Cambridge University, Cambridge, 1980), Chap. 9.

[19]Charles Kittel and Herbert Kroemer, *Thermal Physics,* 2nd ed. (Freeman, San Francisco, 1980), p. 425.

[20]T. Gebele, J. Phys. A **17**, L51 (1984).

[21]G. E. Pike and C. H. Seger, Phys. Rev. B **10**, 1421 (1974).

[22]J. P. Straley, in *Electrical Transport and Optical Properties of Inhomogeneous Media (Ohio State University, 1977),* Proceedings of the First Conference on the Electrical Transport and Optical Properties of Inhomogeneous Media, AIP Conf. Proc. No. 40, edited by J. C. Garland and D. B. Tanner (AIP, New York, 1978), p. 118.

[23]A.-M. S. Tremblay, Shechao Feng, and P. Breton, Phys. Rev. B **33**, 2077 (1986).

[24]L. D. Landau and E. M. Lifshitz, *Fluid Mechanics,* 1st ed. (Pergamon, New York, 1959), p. 27.